Contrib. Mineral. Petrol. 52, 29—55 (1975)

The Orthoenstatite to Clinoenstatite Transformation by Shearing and Reversion by Annealing: Mechanism and Potential Applications

Robert S. Coe
Earth Sciences Board, University of California Santa Cruz, California 95064

Stephen H. Kirby*
Department of Geology, University of California Los Angeles, California 90024

Received February 6, 1975 / May 24, 1975

Abstract. Clinoenstatite (CE) was produced by deforming single-crystal specimens of orthoenstatite (OE) in several different sorts of experiments. Examination with light and transmission electron microscopes shows that the transformation is coherent and involves a macroscopic shear on (100) [001] through an angle of $12.8 \pm 1.3°$, in good agreement with the theoretically expected value of 13.3°, and that the transformation is accomplished by glide on (100) of partial dislocations with $\boldsymbol{b} = 0.83[001]$. Structural analysis provides further insight into the transformation mechanism. Reversion occurs in specimens annealed under a variety of conditions, and thin lamellae of CE in unconstrained, low-strain specimens recover their original shape during transformation back to OE. Our experiments and thermodynamic estimates both suggest that the equilibrium transition temperature is raised roughly 300°C per kilobar of shear stress on (100) [001]. This provides the basis of a method by which it may be possible to determine the magnitude as well as the orientation of the principal stresses that produce CE in nature during deformation of enstatite-bearing rocks.

Introduction

The orthorhombic-monoclinic polymorphic transition in enstatite has been a subject of considerable interest and study since the original discovery by Turner, Heard and Griggs (1960) that orthoenstatite inverts to low clinoenstatite during shear parallel to (100) planes in the [001] direction. Besides being theoretically intriguing from the standpoint of thermodynamics, kinetics and atomic mechanism, this transition may eventually yield information about stress conditions in the earth. Until recently the apparent absence of clinoenstatite in naturally deformed rocks made the question of such an application purely academic. In the past several years, however, clinoenstatite has been identified in a number of mafic and ultramafic bodies (Trommsdorff and Wenk, 1968; Grover, 1972a and b and personal communication; B. W. Evans, personal communication; Frost, 1973), thereby re-opening the possibility of using this transition as a geopiezometer.

A great deal of study has been devoted to the phase relations of the polymorphs of $MgSiO_3$. Much of it is summarized in an extensive review by Smith (1969), so that discussion here is limited mainly to later work dealing with orthoenstatite (OE) and low clinoenstatite (CE).

* Now at U.S. Geological Survey, 345 Middlefield Rd., Menlo Park, California 94025

The very careful hydrothermal study of Grover (1972a and b, and personal communication), in which the OE-CE transformation was reversed at a number of pressures up to 4 kb, establishes CE as the low-temperature phase with a true hydrostatic stability field given by $T = 566°C + (4.5°C/kb)P$. The transformation is very sluggish under these conditions, requiring both the use of fluxes and long reaction times. In striking contrast, the transformation of OE to CE under the appropriate conditions of shear on (100) in the [001] direction takes place very rapidly at temperatures both well above and below the hydrostatic phase boundary, specifically, from at least 20 to 1300°C (Riecker and Rooney, 1967; and Raleigh *et al.*, 1971). The rapid conversion of OE to CE below the hydrostatic phase boundary shows that such shearing has a profound kinetic effect, increasing the reaction rate many orders of magnitude, whereas the transformation above the boundary indicates that the shearing enhances the stability of CE with respect to OE.

A thermodynamic explanation of the enhanced stability of CE suggested by Coe (1970) requires that the OE-CE transition be coherent, reversible, and characterized macroscopically by a uniquely defined transformation strain of simple shear on (100) parallel to [001]. He also proposed a set of atomic displacements in which the coherent transformation of OE to CE would involve a macroscopic angle of shear of 13.3° and result in the orientation relationship of the two polymorphs suggested as most likely by Trommsdorff and Wenk (1968). Transmission electron microscopy of a specimen deformed in the laboratory under known conditions has confirmed this orientation relationship (Coe and Müller, 1973).

In this paper we present experimental evidence concerning the actual value of the angle of transformation shear, the reversibility of the transformation, and details of the transformation mechanism on the atomic scale. Our findings establish the validity of the assumptions required by the thermodynamic theory (Coe, 1970) and confirm and extend greatly the previous results obtained with the transmission electron microscope (TEM) (Coe and Müller, 1973; Müller, 1974). Then, on the basis of the theory, we make rough estimates of the quantitive effect of shear stress on the temperature of the transition, and discuss how, if the temperature and mean pressure during deformation are independently known, this may eventually enable us to estimate the stress fields which produced CE in nature.

Experimental Results and Discussion

Orthoenstatite to Clinoenstatite

High-Pressure Deformation Experiments. Starting specimens were cylinders about 0.6 cm in diameter and generally 1.8 cm long cored out of large, massive cleavage chunks of single-crystal OE from Bamble, Norway. The cores were drilled at about 45° to the *c*- and *a*-axes, so that axial compression would achieve maximum resolved shear stress on (100) planes in the direction of [001]. Measurement on the universal stage showed that $2V_\alpha$ is around 86°, suggesting that about 14 mole percent of orthoferrosilite is in solid solution (Deer *et al.*, 1963). Electron probe analyses confirm this supposition, yielding an idealized formula ($Mg_{0.854}$ $Fe_{0.141}$

$Ca_{0.005})SiO_3$. Al was not detectable in significant amount, and the sum of the mole percents of other likely cations was less than that for Ca. Thus the specimens fall in the bronzite field just outside the enstatite compositional range, but nonetheless we shall still call them OE for simplicity since they appear to undergo the same transformation under shear as the pure magnesium end member. This is not unexpected because the pure iron end member, orthoferrosilite, is isomorphous with OE and transforms under shear to the isomorphous monoclinic polymorph, clinoferrosilite (Lindsley and Munoz, 1969; and Smith, 1969).

All deformation experiments were conducted in Griggs-type solid-medium apparatuses (Green, Christie, and Griggs, 1970). Eight runs were at 800 °C and used talc as a confining medium. The confining pressure was 5 kb for six runs and 15 kb for the other two, and the strain rate was approximately 10^{-4} sec^{-1} for five of the runs and 10^{-5} sec^{-1} for the other three. Six of the specimens were split in half and polished on the axial plane parallel to (010). Both halves were scribed with an orthogonal grid either parallel or at 45° to the *a*- and *c*-axes, and re-joined with a thin (0.0025 cm) piece of tantalum or plantinum foil between them. This enabled us to observe the distribution of strain in these specimens. Finally, four additional runs were performed at room temperature and 15 to 19 kb on polished prisms of OE in sample assemblies with an inner liner of polyvinyl chloride (PVC) as as a pressure medium. The purpose of these runs was to suppress deformation by slip in order to measure the angle of transformation shear. These specimens were also used to study the reverse transformation in annealing experiments.

The deformation procedure was to bring the confining pressure P and temperature T up to the desired value, shorten the specimens by various amounts at constant strain rate, and then drop in turn the load, pressure and temperature. CE was produced in all specimens, and no evidence of reversion of CE to OE could be detected in these runs at 800 °C or less. During deformation at 800 °C the differential stress rose quickly once the specimen was encountered until an apparent yield point was reached between 3 to 5 kb. This was not a true yield point in the strict sense of the word because the specimen had already permanently shortened by 2 to 3 percent, but nonetheless the rate of increase of differential stress dramatically slowed at that point. The stress at which the yield occurred was about the same regardless of whether the strain rate was 10^{-4} or 10^{-5} sec^{-1}, but it rose to values ranging from 7 to 14 kb for the runs at room temperature. In some runs carried to large enough strains there was a second strain-hardening stage in which the rate of increase of differential stress rose markedly when the shortening exceeded a critical value of about 10 to 11 percent. This was observed in the runs at 5 kb confining pressure in talc and 17 kb in PVC, but not in those at 15 kb in talc.

Optical Microscopy. These features of the stress-strain record described above can be related to thin sections of specimens deformed to varying strains (Fig. 1). Specimens of OE shortened about 4 percent or more all show direct lamellae of CE parallel to (100) and a CE-containing kink which trends at a high angle to them (Fig. 1, left). The CE referred to in this paper has been identified variously by optical properties (high birefringence in (010) sections and $\boldsymbol{Z} \wedge \boldsymbol{c} \cong 32°$), X-ray

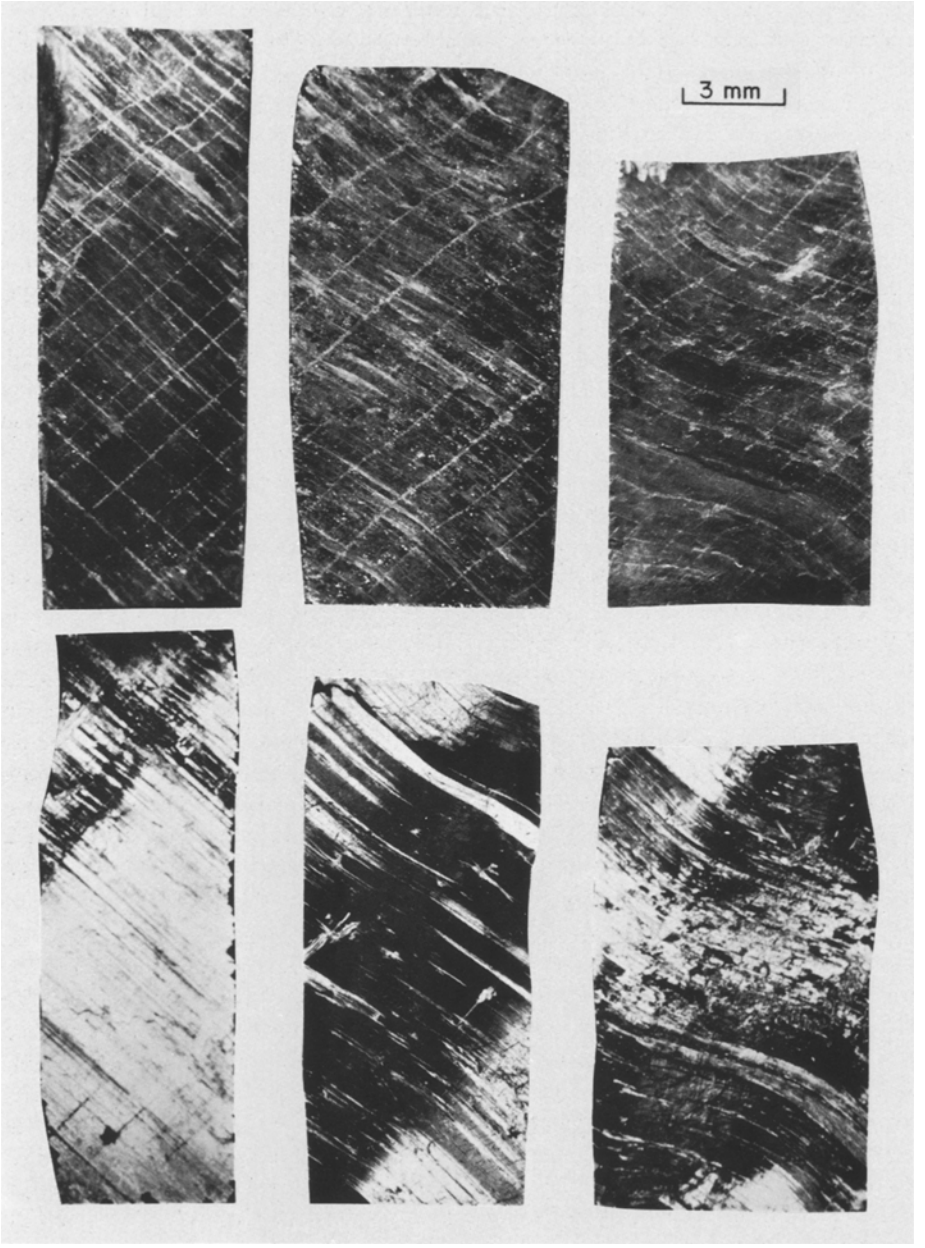

Fig. 1. (010) sections of deformed cores of Bamble enstatite with *c*-axis NW-SE: (top) polished axial sections showing plane strain defined by scribed grid (see text); (bottom) corresponding thin sections under crossed nicols showing CE at extinction. (Left) 4 percent shortening at 10^{-4} sec^{-1}, 800° C; (center) 14 percent shortening at 10^{-4} sec^{-1}, 800° C; (right) 22 percent shortening at 10^{-5} sec^{-1}, 800° C, followed by accidental heating to $\sim$ 1200° C for $\sim$ 30 sec during shutdown (note patchy light areas of OE in the center that resulted by reversion of CE)

powder and single crystal diffraction patterns, and single-crystal electron diffraction patterns. As has invariably been found in the past, the OE and CE have b-, c-, and a^*-axes in common and are in contact on (100) planes. Almost always in low-strain specimens both the highest concentration of direct lamellae and the kink occur in the lower portion of the specimen, emanating from the bottom corners and intersecting in a cross about 1/4 of the way up the specimen. We believe the direct lamellae form first during deformation, and that the apparent yield point at about 2 to 3 percent strain marks the beginning of formation of the kink .As shortening continues, transformation of more OE to CE is accomplished by the simultaneous growth of the kink band and growth of the direct lamellae outside the kink. At around 10 to 11 percent strain most of the specimen, except triangular patches at either end which are hindered from shearing by the rigid end pieces, has transformed to CE, and further deformation is accomplished mainly by slip in CE (Fig. 1, center). This change in the deformation mechanism probably accounts for the increase in rate of rise of differential stress observed in the runs at 10 to 11 percent strain. The apparent absence of this phenomenon in the runs in talc at higher confining pressure may be due to the masking effects of higher friction. Of course, this description is undoubtedly over-simplified; it is very likely that slip begins in CE in some places while transformation is still proceeding elsewhere.

Study of the deformed grids of Fig. 1 and measurement of the deformed specimens allow us to further characterize the deformation. The dominant macroscopic strain is simple shear on (100) parallel to [001], but it is inhomogeneously distributed. The combination of direct shear and shear by kinking is almost sufficient to satisfy the mechanical constraints that the ends of the specimen remain parallel and centered over each other. Transformation to CE is always associated with deformation of the corresponding portion of the grid, and is optically incomplete (lower birefringence and lower apparent $\boldsymbol{Z} \wedge \boldsymbol{c}$ in (010) sections) in regions of low strain and complete in regions of high strain.

Attempts to use the grids to determine the angle of shear associated with the transformation are complicated by the fact that the grids are too crude and too widely spaced to define precisely the inhomogeneous shear that occurred. Another difficulty is that at elevated temperatures the CE was formed in regions that vary greatly in amount of macroscopic shear, presumably because of varying amounts of deformation by slip. The minimum angle of shear associated with *complete* transformation, however, was $\psi = 10$ to $15°$ as measured under the microscope where a grid line parallel to the a-axis of OE could be followed into a lamella of CE. The same range for ψ was also estimated from the minimum angle of rotation ω of (100) traces in kink bands containing optically pure CE according to the formula for ideal kinking: $\tan\psi = 2\tan(\omega/2)$ (Weiss and Turner, 1972).

More precise measurements of the transformation shear have been accomplished by another method. Rectangular prisms of OE with polished faces were deformed at room temperature in order to suppress slip. The polished surfaces were rotated in bands parallel to the trace of (100), and thin sections showed these to be lamellae of CE (Fig. 8). As expected, no glide band rotations were noted on (010)

polished surfaces. The smaller of these bands displayed nearly identical rotations, whereas the larger ones were more complex and had larger, variable rotations on the average because of additional deformation by slip. The angle of shear corresponding to the rotation of the polished surface by the small lamellae is $12.8 \pm 1.3°$, in fairly good agreement with the value of 13.3° predicted by the model proposed earlier by Coe (1970).

Transmission Electron Microscopy. There have been published recently a considerable number of studies by transmission electron microscopy (TEM) of orthopyroxenes which bear lamellae of various sorts of clinopyroxene (Lally *et al.*, 1972; Green and Radcliffe, 1972; Boland, 1972 and 1974; Champness and Lorimer, 1973, 1974; Lorimer and Champness, 1973; Coe and Müller, 1973; Kohlstedt and Vander Sande, 1973; Buseck and Iijima, 1974; Vander Sande and Kohlstedt, 1974; Müller, 1974). In this section we discuss the defects observed in OE and CE after deformation of the parent OE, with particular emphasis on the partial dislocations and stacking faults which appear to accomplish the phase transformation (see also Kirby, 1975, for fuller treatment).

Thin foils 2 to 3 mm in diameter were prepared for study by TEM by ion bombardment of selected portions of thin sections. Most foils were from the split, scribed cores, so that the average shear strain that these foils underwent is known. The foils were of two orientations: (010), in which the foil is normal to the *b*-axis; and off-(100), in which the foil contains the *b*-axis and is inclined about 20° to (100). The micrographs which follow are all from specimens deformed in talc assemblies at 800 °C.

Fig. 2 shows bright-field (BF) electron micrographs from four (010) foils in which the angle of shear strain γ varies from less than 3 to 32°. In each a diffraction pattern taken directly along the [010]-zone axis is included, and the diffracting vector corresponding to the bright-field micrograph is shown. When $\gamma < 3°$ (Fig. 2A) the diffraction pattern is indistinguishable from pure OE and only a few thin lamellae of CE are present. Some of the lamellae terminate in packets of partial dislocations on the system (100)[001] (Table 1), and there are few isolated unit dislocations. When $\gamma \cong 7°$ shear (Fig. 2B) the diffraction pattern is streaked parallel to a^* and is a mixture of those for both OE and CE, roughly 50 percent of the specimen having transformed to lamellae of CE. There are still few isolated unit dislocations. When $\gamma = 15°$ (Fig. 2C) the diffraction pattern is unstreaked and corresponds to pure untwinned CE. The specimen is almost all CE with only a few residual lamellar features. In this specimen there are plentiful isolated unit dislocations on the slip system (100) [001] (Table 1). Thus we see again that transformation takes place first with little or no slip until the transformation shear of 13.3° is exceeded, after which deformation is accomplished chiefly by slip in CE. This is further borne out by the last micrograph with $\gamma = 32°$ (Fig. 2D), which differs from the previous one chiefly in that there are regions of both very high and fairly low dislocation intensity.

Fig. 3 shows BF micrographs of three foils with the off-(100) orientation in order of increasing strain. This orientation affords an especially good view of the defects of greatest interest. The foil of Fig. 3A is almost unsheared OE, showing a relatively low density of stacking faults and associated partial dislocations of

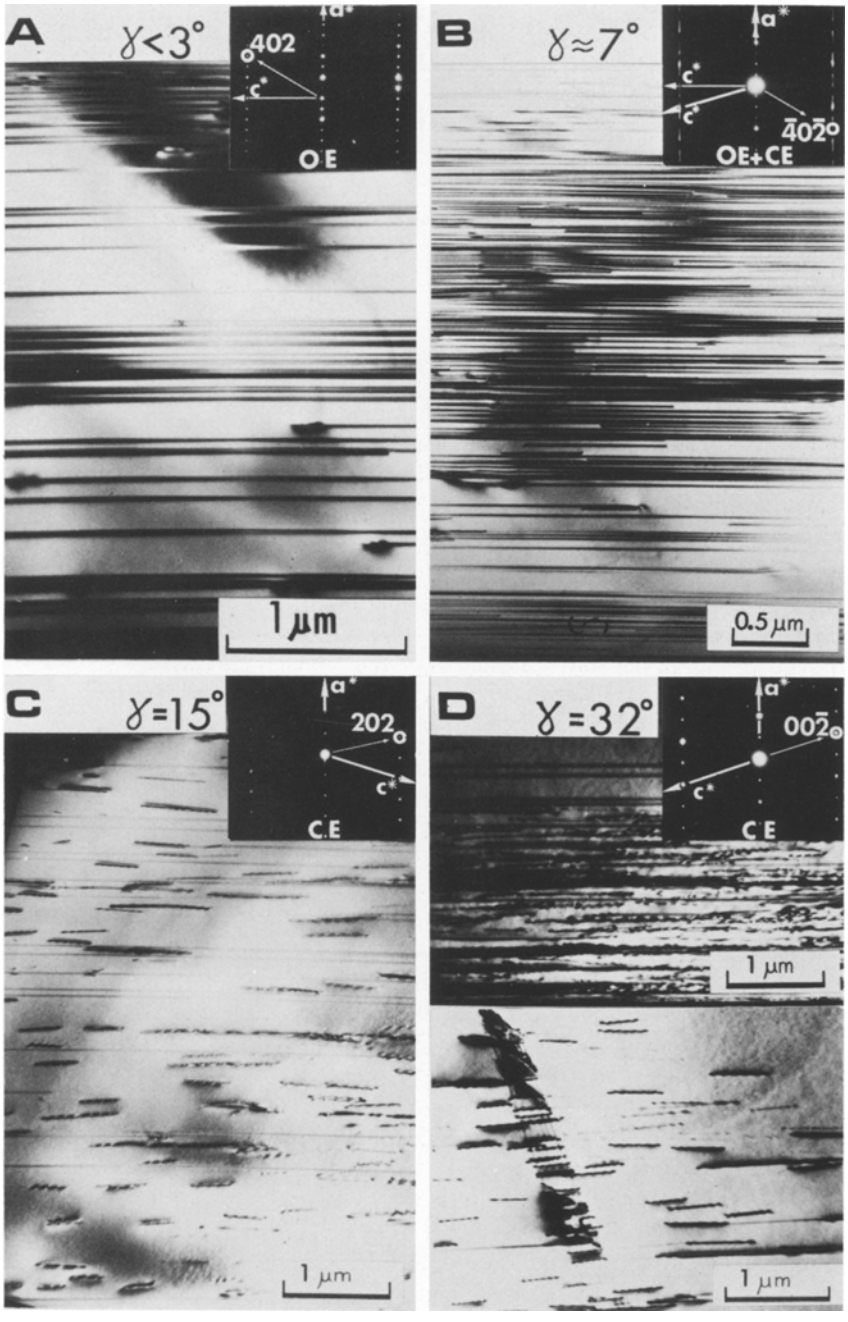

Fig. 2A—D. BF electron micrographs and associated diffraction patterns of (010) foils from deformed specimens of Bamble OE. Thin arrow pointing to circled spot indicates diffraction vector $\boldsymbol{g}$. Note increase in proportion of CE with increasing angle of macroscopic shear (γ) of foil. See text for full discussion

Table 1. Summary of contrast observations of defects produced by deformation or annealing

Sample history	Phases	Defect	Orientation	Conditions for contrast	Conditions for out of contrast	Glide system
Low strain ($\gamma > 13°$)	OE CE	Stacking[a] faults	(100)	(202)[c], (302)[c]	(020)[c], (040), (060)[c], (080), (610)[c]	(100) [001] $\boldsymbol{R} = 0.83$ [001]
		Partial[a] dislocations	variable; often ⟨012⟩, [001], [010]	(202)[c], (302)[c]	(020)[c], (040), (060)[c], (080), (200), (400), (600), (800)[c]	(100) [001] $\boldsymbol{b} = 0.83$ [001]
		Partial dislocations	[001]		(202)[c], (302)[c], (020)[c], (040), (060)[c]	(100) [001] $\boldsymbol{b} = 0.17$ [001]
High strain ($\gamma > 13°$)	CE	Unit[a] dislocations	$\sim$⟨012⟩	($\bar{2}02$)[c], (202)[c], (402)[c], ($\bar{4}02$)[c], (002)[c], ($\bar{1}02$)[c], ($\bar{2}22$)[c]	(200), (400)[c], (600)[c], (800)[c], (020)[c], (040), (060)[c]	(100) [001]
		Unit dislocations	[001][b] [010]	(060)[c], (020)[c]	($\bar{2}02$)[c], (202)[c], (402)[c], ($\bar{4}02$)[c], (002)[c], ($\bar{1}02$)[c], (200), (400)[c], (600)[c], (800)[c]	(100) [010]
		Partial dislocations	Variable	($\bar{2}02$)[c], (202)[c], (402)[c], ($\bar{4}02$)[c], (002)[c], ($\bar{1}02$)[c]	(200), (400)[c], (600)[c], (800)[c], (020)[c], (040), (060)[c]	(100) [001] $\boldsymbol{b} =$? [001]
		Stacking[a] faults	(100)	($\bar{2}02$)[c], (202)[c], (402)[c], ($\bar{4}02$)[c], (002)[c], ($\bar{1}02$)[c]	(020), (040)[c], (060)[c]	(100) [001] $\boldsymbol{b} =$? [001]
Deformed to CE + annealed at $T \geq 1100°$ C	OE	Unit[a] dislocations	[001] to curved	(202)[c], (302)[c]	(200), (400), (600), (800)[c], (020)[c], (040), (060)[c]	(100) [001]
		Unit dislocations	[001]	(020)[c], (060)[c]	(202)[c], (302)[c]	(100) [010]
		Partial dislocations	Variable; often [010], [001]	(202)[c], (302)[c]	(200), (400), (600), (800)[c], (020)[c], (040), (060)[c]	(100) [001] $\boldsymbol{b} =$? [001]
		Stacking[a] faults	(100)	(202)[c], (302)[c]	(020)[c], (060)[c], (080)	100 [001] $\boldsymbol{R} =$? [001]

[a] Most prominent defects.
[b] Dominant direction.
[c] Extinction distance < 5000 Å.

the system (100) [001] (Table 1). Such defects have been described before in both artificially and naturally deformed orthopyroxenes (Green and Radcliffe, 1972; Coe and Müller, 1973; Kohlstedt and Vander Sande, 1973). When $\gamma = 6°$ (Fig. 3B) OE and CE are present in roughly equal amounts and there is an increased density

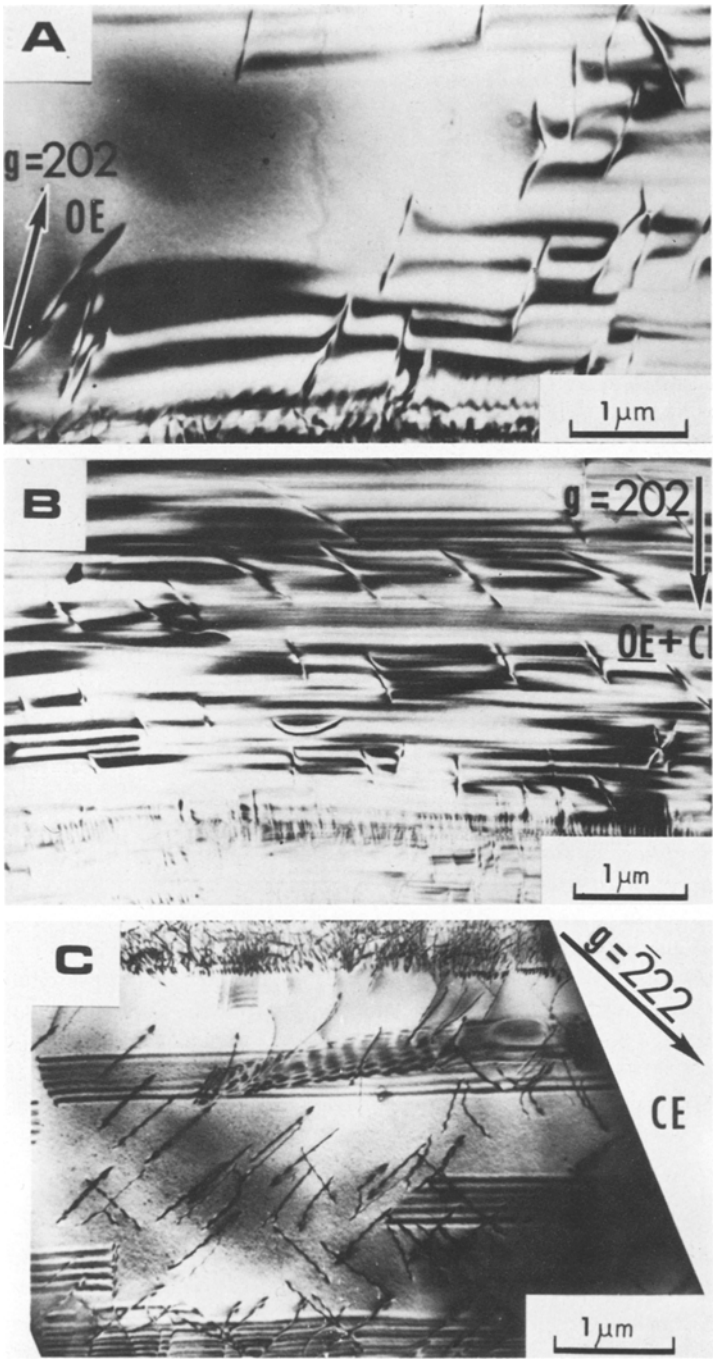

Fig. 3A—C. BF electron micrographs of off-(100) foils of deformed specimens of Bamble OE in order of increasing angle of macroscopic shear (γ): (A) $\gamma < 2°$, (B) $\gamma \simeq 6°$, (C) $\gamma \simeq 30°$. [010] is E-W and arrows denote diffracting vector. See text for full discussion

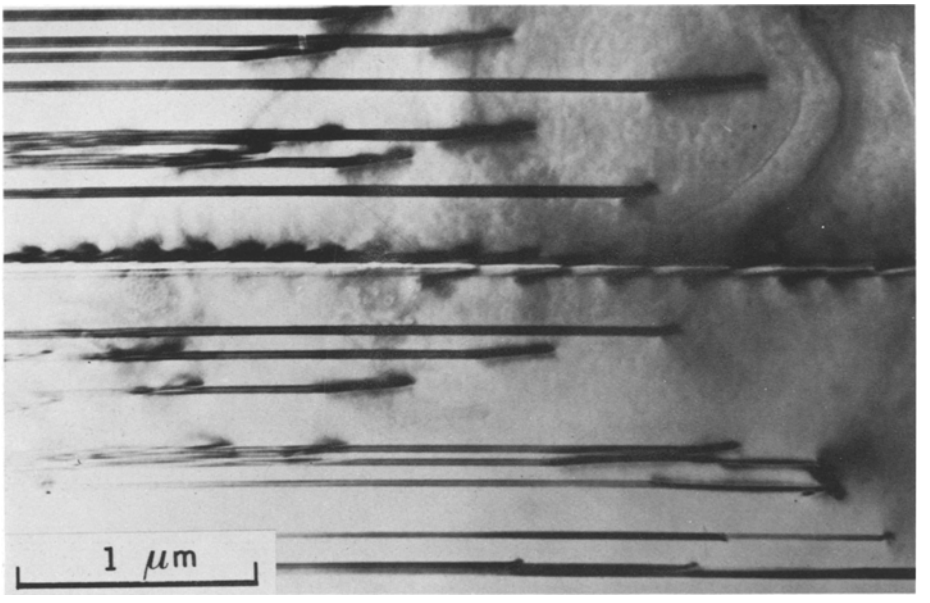

Fig. 4. BF electron micrograph of (010) foil of deformed Bamble OE tilted about [001] (E-W), showing isolated stacking faults with associated partial dislocations and a lamella of CE (bright, near center). Note how CE lamella thickens from right to left (presumably due to the transformation partials visible on the lamella boundary—see text and Fig. 5).

of CE lamellae, overlapping stacking faults, and associated partial dislocations. The foil of Fig. 3C is sheared about 30° and shows pure CE. There are only a few residual stacking faults, but numerous unit dislocations with Burgers vector parallel to [001] and dislocation lines approximately parallel to ⟨012⟩ (Table 1), some of which can be seen to form loops that lie in the (100) glide planes. A band containing dense tangles of unit dislocations is shown at the top of Fig. 3C.

The stacking faults and associated partial dislocations in low strain specimens must be intimately associated with the transformation because they are numerous when transformation is taking place and almost disappear when it is complete. Moreover, the system (100) [001] to which they belong is just the right one to accomplish the macroscopic strain of the coherent transformation. Thus we would expect to see these partial dislocations in the boundaries of lamellae of CE in OE. Such is the case in the (010) foil of Fig. 4, where the partial dislocations on the top and bottom surfaces of the lamella in the center of the micrograph accomplish the thickening of the lamellae that is observed from right to left. Repeated measurements show that on the average about 15 ± 5 Å is added to the CE lamella in the $\boldsymbol{a}^*$ direction per defect, which is what would be expected in any transformation mechanism in which CE is produced by shearing or "untwinning" alternate 9 Å subcells of OE (Turner *et al.*, 1960; Brown *et al.*, 1961; Coe, 1970). That is, each partial dislocation should add 18 Å in thickness to the CE lamella in the $\boldsymbol{a}^*$ direction, as illustrated schematically in Fig. 5. Recently Müller (1974) has demonstrated by lattice imaging with the TEM that CE lamellae

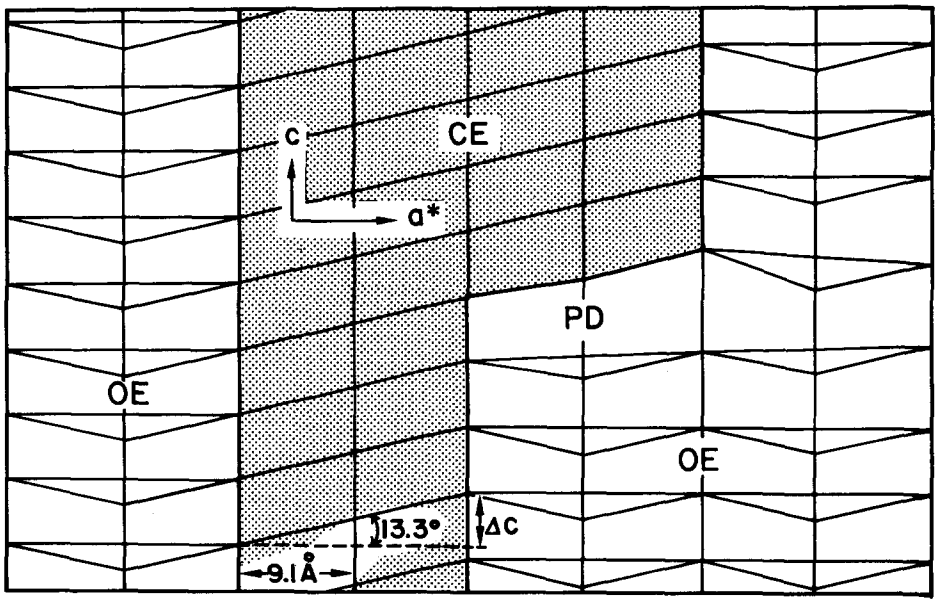

Fig. 5. Lamella of CE (stippled) in host of OE. 9.1 Å wide subcells compose both the OE and CE phases. The stacking fault displacement Δc is the offset of the OE across the 18.2 Å lamella of CE which would happen during transformation by "untwinning" one of the OE subcells (see Fig. 6 and 7). The lamella thickens by 18.2 Å upwards through addition of another stacking fault bounded by a partial dislocation (*PD*) with $\boldsymbol{b} = 0.83[001]$ (see text). Glide of these partials on (100) accomplishes the transformation

formed by shearing OE always consist of an even number of 9 Å lattice units parallel to $\boldsymbol{a}^*$, another clear consequence of the "untwinning" mechanism.

In the following paragraphs we present the principal results of extensive diffraction contrast experiments on isolated stacking faults and partial dislocations. [A full analysis will appear elsewhere (Kirby, 1975).] These isolated defects appear similar to those which occur in the boundaries of CE lamellae, and we interpret them to be isolated lamellae of CE only 18 Å thick. Thus, the displacement vector of these stacking faults should be essentially that required to transform OE to CE.

Stacking faults usually produce contrast consisting of characteristic fringes when viewed by TEM, and with sufficient data the displacement vector $\boldsymbol{R}$ of the stacking fault may be estimated (see Amelinckx, 1970, for review). Of particular interest is the phase angle $\alpha = 2\pi \boldsymbol{g} \cdot \boldsymbol{R}$, where $\boldsymbol{g}$ is the diffracting vector. If α is zero or an even multiple of π, then no contrast results. The conditions for no contrast listed in Table 1 for the stacking faults are consistent with $\boldsymbol{R}$ being parallel to [001].

If α is an odd multiple of π, particularly distinctive fringes are produced: fringes are symmetrical in both bright field (BF) and dark field (DF), BF and DF fringes are complementary, and new fringes are added at the sides of faults where they cross thickness extinction contours. These characteristics are observed in

faults when $\boldsymbol{g}=(202)$ (Kirby, 1975). Since $\boldsymbol{R}$ is parallel to [001], its magnitude R can be found approximately by the condition $\alpha=2\pi\boldsymbol{g}\cdot\boldsymbol{R}=4\pi R=(2n+1)\pi$, or $R=(2n+1)/4$. Kirby (1975), following the general method of Amelinckx (1970), has shown by detailed calculations for enstatite that the observed characteristics of the fringes would persist for values of R which range 0.125 above or below $(2n+1)/4$. The stacking fault represented by a single 18 Å lamella of CE involves a displacement vector with magnitude $R=\Delta c/c=(18.2/c)\tan(13.3°)=0.83$ if it is formed by the 13.3° transformation mechanism (see Fig. 5). This lies within the bounds imposed by diffraction contrast theory for $n=1$: *viz.*, $0.625<R<0.875$. Hence $\boldsymbol{R}=0.83\,[001]$ is the likely stacking fault displacement vector. Kohlstedt and Vander Sande (1973) observed similar stacking faults in naturally deformed orthopyroxene for which they concluded $\boldsymbol{R}=1/4$ [001] (i.e., $n=0$). However, since $n=1$ appears to satify their observations as well, it may be that those stacking faults are the same as the ones that we observe that are related to the phase transformation.

Detailed study of the partial dislocations bounding isolated stacking faults further support and extend these conclusions (Kirby, 1975). When both bounding partials are visible in the same micrograph with $\boldsymbol{g}=(202)$, one is always in strong and the other in weak contrast. This would arise very naturally if the partials are formed by dissociation of unit dislocations by the reaction $[001]\rightarrow 0.83\,[001]+0.17\,[001]$. Both isotropic theory and computer-simulated images using the anisotropic properties of enstatite indicate that the "weak" partials ($\boldsymbol{b}=0.17$ [001]) are out of contrast for $\boldsymbol{g}=(202)$. The simulations also suggest that the Burgers vector of the "strong" partials cannot exceed unity, for when it does the "beaded" character of the simulated partials (which is what we actually observe with the TEM) gives way to straight dark and bright lines.

The "strong" partials are by far the most numerous in micrographs of low-strain specimens and invariably terminate the leading edges of propagating CE lamellae. This, together with the correspondence between $\boldsymbol{R}$ predicted by the 13.3° "untwinning" mechanism and that inferred from fault contrast, indicates that these strong partials with $\boldsymbol{b}=0.83\,[001]$ transform OE to CE by glide on (100). We disagree with Boland's (1974) suggestion that the transformation partials have $\boldsymbol{b}=1/4\,[001]$.

It is not clear why the "weak" partials appear so less numerous. The explanation may be that they are obscured in (001) networks of unit dislocations in the starting material where they are created by dissociation (Kirby, 1975). The "weak" partials are expected to be immobile because they do not produce a locally stable structure, hence they would remain in the (001) networks after they formed. The "strong" and "weak" partial dislocations we have observed may be the same as those in micrographs of naturally deformed orthopyroxenes published in the recent literature (Green and Radcliffe, 1972; Kohlstedt and Vander Sande, 1973). Kohlstedt and Vander Sande (1973) have suggested that these partials have $\boldsymbol{b}=1/4\,[001]$.

Structural Analysis. The transformation mechanism involves shear on (100) parallel to [001] on the macroscopic scale and results in a particular orientation relationship of CE in OE with a^*-, b- and c-axes in common. Thus the most

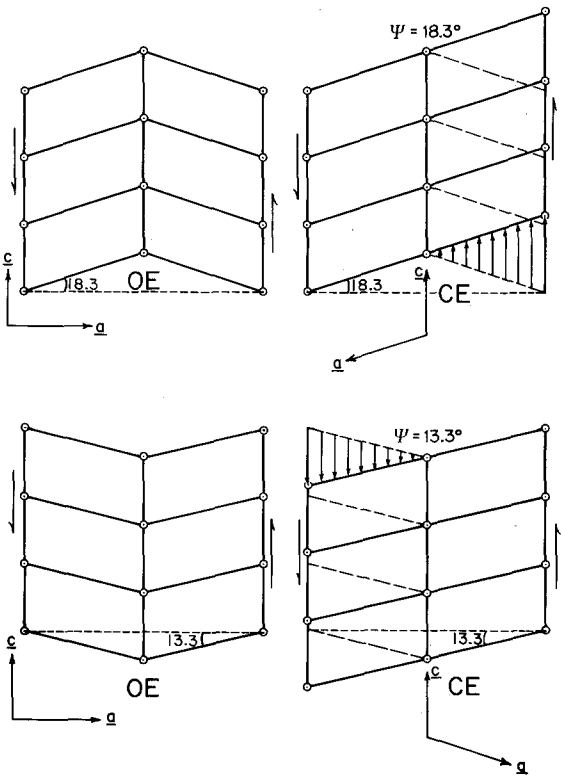

Fig. 6. Geometry of two coherent mechanisms that would accomplish transformation of OE to CE by "untwinning" different subcells of OE. Note different angles of transformation shear (ψ) and orientations of CE that are produced by the two mechanisms for a given sense of shear (arrows). Several lines of evidence support the 13.3° mechanism (see text)

attractive mechanisms from a structural standpoint are those which involve translations of the Si chains parallel to *c*, thereby breaking none of the strong Si-O bonds. Fig. 6 illustrates the two principal mechanisms of this type that have been proposed, one involving a macroscopic shear of 18.3° (Brown *et al.*, 1961) and the other 13.3° (Coe, 1970). For a given sense of shear on (100) parallel to [001] the two mechanisms entail shearing of alternate slabs of OE which are parallel to (100) and about 9 Å thick, leaving the other slab virtually unaffected. Each mechanism "untwins" a geometrically different subcell of OE in one or the other of the alternating slabs. For purposes of comparison, however, we can consider the effect of shearing in *opposite* senses on the *same* slab of OE, one sense corresponding to the 18.3° mechanism and the other to the 13.3° mechanism (Coe, 1970, Fig. 2; and Fig. 7, this paper). As already noted, the shear angle and orientation relationship actually observed are consistent with the 13.3° mechanism.

The atomic displacements that we think accomplish the transformation are illustrated in Fig. 7. Displacements parallel to $\boldsymbol{a}^*$ are very small, hence $\boldsymbol{a}^*$ projections are used to display atomic positions. Only oxygen and magnesium positions are plotted.

To a first approximation the OE-CE transformation mechanism may be thought of as a restacking produced by shearing the oxygen sheets in half of the octahedral layers parallel to [001] from one close-packed configuration to the next. The sense

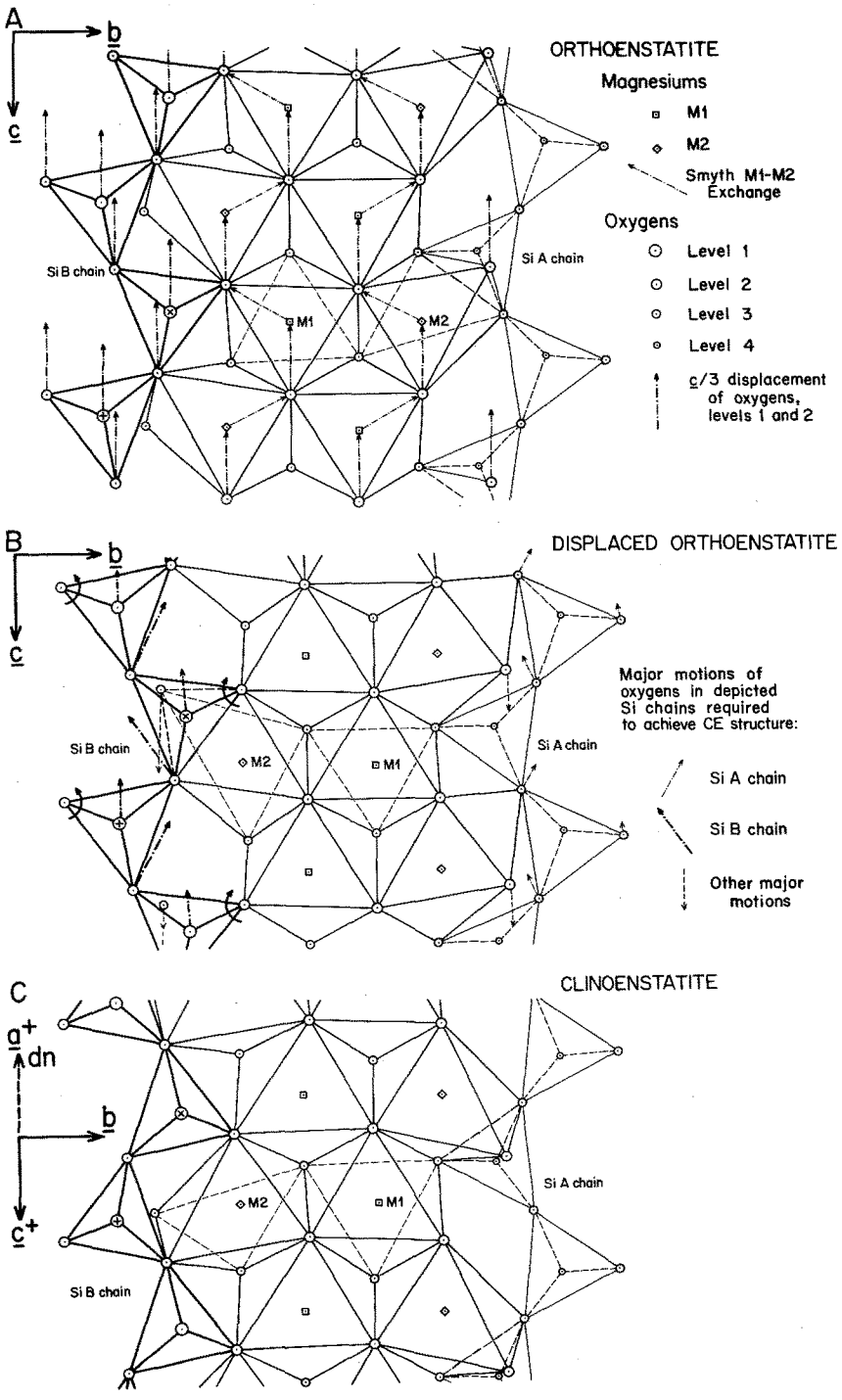
A
b
c
ORTHOENSTATITE
Magnesiums
M1
M2
Smyth M1-M2 Exchange
Oxygens
Level 1
Level 2
Level 3
Level 4
c/3 displacement of oxygens, levels 1 and 2
Si B chain
Si A chain
M1
M2
B
b
c
DISPLACED ORTHOENSTATITE
Major motions of oxygens in depicted Si chains required to achieve CE structure:
Si A chain
Si B chain
Other major motions
Si B chain
Si A chain
M2
M1
C
a+
dn
b
c+
CLINOENSTATITE
Si A chain
M2
M1
Si B chain

of shear indicated in Fig. 7A is that consistent with the 13.3° mechanism, and it is important to note that with this sense there is minimum interference between the oxygens during displacement. On the other hand, the 18.3° mechanism requires the opposite sense of shear for which the interference of oxygen atoms is most severe and the displacement twice as large. We believe this is the reason that the 13.3° mechanism occurs in preference to the 18.3° mechanism. It would also appear to offer an explanation for why protoenstatite reverts metastably to polysynthetically twinned CE when cooled quickly into the OE stability field (Brown *et al.*, 1961; Smyth, 1974); there is no way to achieve the OE structure from protoenstatite by shearing of octahedral layers parallel to [001] without severe oxygen interference unless the sense of shear reverses itself in adjacent 9 Å slabs. We would expect non-uniform thermal stresses to develop during rapid cooling of a crystal to which no external stress is applied, but it is extremely unlikely that the shear stress on (100) parallel to [001] would alternate in sense with just the periodicity required to favor the formation of OE. Any other pattern of alternating shear stresses would favor the formation of twinned CE.

For a perfectly close-packed octahedral layer the relative displacement of oxygen sheets would be 1/3[001] in the sense of the 13.3° mechanism and 2/3 [001] for the 18.3° mechanism. The former displacement is indicated by arrows in the OE structure of Fig. 7A, and the resultant sheared structure is shown in Fig. 7B. There are two octahedral layers per 9 Å slab, so that the total displacement per unit repeat distance of OE caused by the shearing is 2/3[001]. The remainder of the displacement (0.83[001] total is required for the 13.3° mechanism) is brought about by additional movements of the tetrahedral chains, which ease the distortion of the M2 octahedral sites and eliminate the additional edge sharing of Si-B tetrahedra with M2 octahedra in the hypothetical sheared structure. These displacements, which are indicated by arrows in Fig. 7B, complete the transformation to CE (Fig. 7C) except for very minor readjustments of atomic positions. It should be kept in mind, however, that our division of the transformation displacements into two distinct stages is simply a device to clarify the description. In all probability the actual structure during transformation never coincides with the hypothetical sheared structure of Fig. 7B.

Although no Si-O bonds are broken by the atomic movements postulated above, some Mg-O bonds must be broken during shear of the octahedral layers. In the original 13.3° mechanism these cations move parallel to [001] in the same sense as the macroscopic shear (Coe, 1970), half of the original Mg-O bonds are broken, and M1- and M2-cations in OE move to M1- and M2-sites, respectively, in CE. Smyth (1974) has proposed a modification in which M1-cations move to

Fig. 7A—C. Proposed atomic displacements for the coherent transformation of OE to CE (13.3° mechanism). The dominant displacements of oxygens can be visualized as shear of octahedral layers by 1/3[001] (arrows in A) to a hypothetical transitional structure (B), followed by rotations of silicon tetrahedra and a few other related major displacements of octahedral oxygens (arrows in B) to achieve the CE structure (C). Each 9 Å slab parallel to a^* contains two octahedral layers, and transformation involves shearing both layers in alternate 9 Å slabs (the other slabs remaining unsheared)

M2-sites and *vice-versa* (Fig. 7A). We favor Smyth's displacements (Fig. 7A) to those of the original 13.3° mechanism because they require breaking only one-third of the original Mg-O bonds and involve less apparent interference of Mg-cations with impinging oxygens. Whether the exchange of cation sites that is required actually occurs can and should be tested: the ordering of Fe and Mg ions M1- and M2-sites should reverse in orthopyroxenes transformed to the CE structures by shear.

A few points in the literature on transformation mechanisms need correcting. Smyth (1974) states that the mechanism of Sadanaga *et al.* (1969) and Coe (1969) are the same, but in fact they are very different. The former is essentially the 18.3° mechanism of Brown *et al.* (1961), except that the relative displacements of adjacent Si-B chains is different in sense and larger in magnitude. Also, the displacement of M-cations in the 13.3° mechanism of Coe is in the opposite sense as that stated by Smyth and depicted in his Fig. 3. Finally, we disagree with the statement by Boland (1974) that the transformation is accomplished by the propagation of partial dislocations with $\boldsymbol{b} = 1/4\,[001]$. We can see no way to obtain the CE structure by displacing the OE structure on planes parallel to (100) by 1/4 [001]. Moreover, for reasons identical to those discussed above with regard to partials with $\boldsymbol{b} = 0.17\,[001]$, we would not expect such dislocations to be mobile because of the high energy of the associated stacking faults.

Clinoenstatite to Orthoenstatite

Reversion at 1 atm Pressure. An important unanswered question has been whether or not the transition could be truly reversed; that is whether the original shape is recovered during transformation from CE back to OE. The thermodynamic treatment of the effect of shear stress on this transition (Coe, 1970) depends formally on the assumption that this is possible.

To test for reversibility of the shape change we heated CE contained in polished specimens which had been used in the experiments to determine the angle of the transformation shear. The CE lamellae showed up as bands parallel to the trace of (100) where the polished surface had been rotated by the transformation shear. The crystals were sealed in glass tubes with steel wool to prevent oxidation of the iron and were unconstrained (external shear stresses zero). After heating several hours at 1000°C there were faint signs of reversion, and after heating at 1100°C for 5 hrs the narrowest bands of CE had disappeared, their surfaces having rotated back to the original planar polished surface (Fig. 8). Thus for these thin bands of CE the transition was definitely reversed. The surfaces of the wider bands of CE became less distinct during the reversion to OE, but did not entirely disappear. This is to be expected because these bands are thought to have undergone shear by both transformation and slip. Only the transformation shear could be recovered by reversion to OE.

Reversion at High Pressure. In five runs in talc set-ups at 800°C and confining pressures of 5 to 15 kb in which transformation to CE must have occurred throughout the major part of the specimen because the shear exceeded that required for transformation, the differential compressive stress was dropped to zero after deformation and the specimen was "annealed" at a higher temperature between 950 and 1200°C for times ranging from a few minutes to a few hours. For these

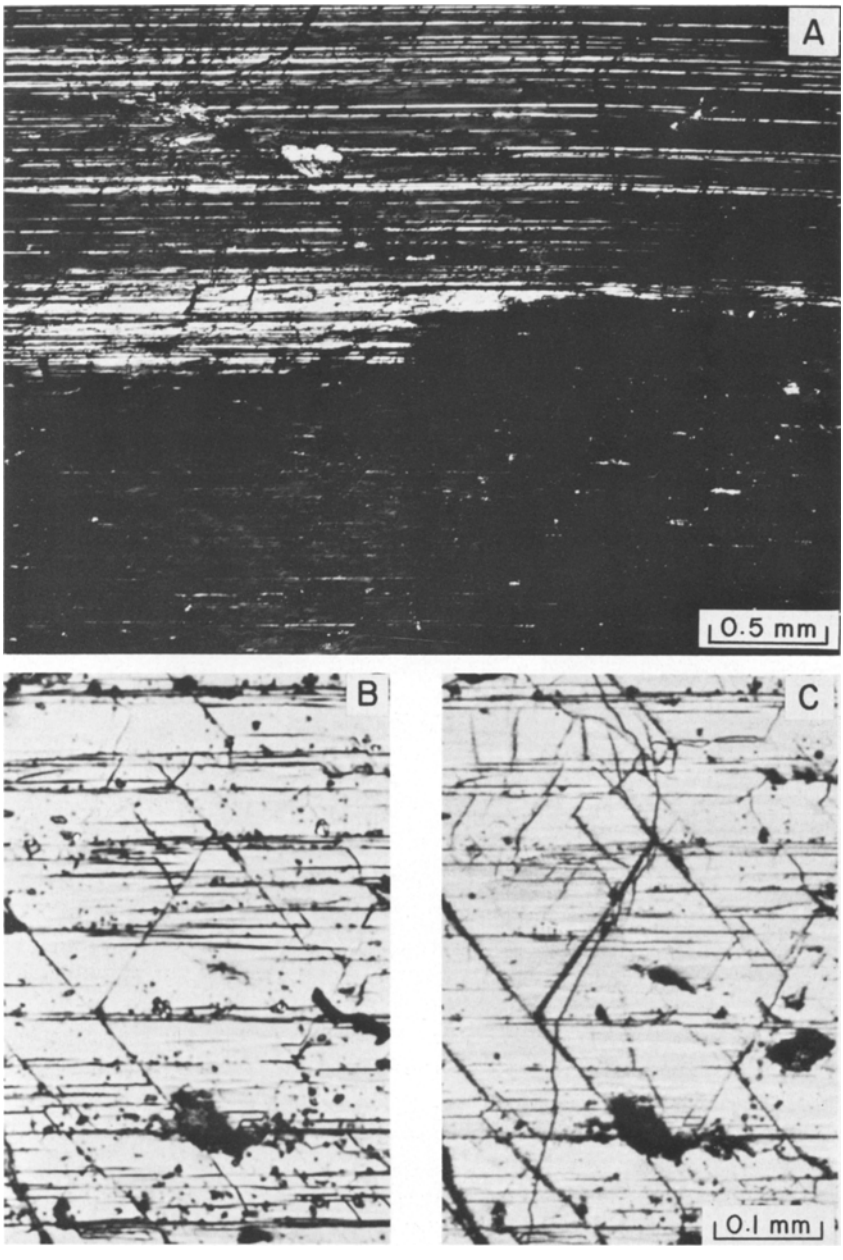

Fig. 8A—C. Reversion of CE to OE by annealing at zero pressure of polished specimen previously shortened by 6 percent at 10^{-4} sec^{-1}, 20° C and 17 kb. (A) (010) thin section under crossed nicols of two pieces rejoined after annealing at 1000° C for 200 min (top) and 1100° C for 300 min (bottom). There is very little reversion at 1000° C and almost total reversion at 1100° C (c-axis and CE lamellae E-W, OE at extinction). (B) Original polished surface under reflected light of same specimen as 8A but at 45° to *a* and *c* E-W dark lines are rotated bands containing lamellae of CE (see text). (C) Same surface as (B) after annealing at 1100° C for 300 min. Note many of the dark bands containing CE have become lighter and a few have disappeared entirely as a result of rotating back during reversion to OE

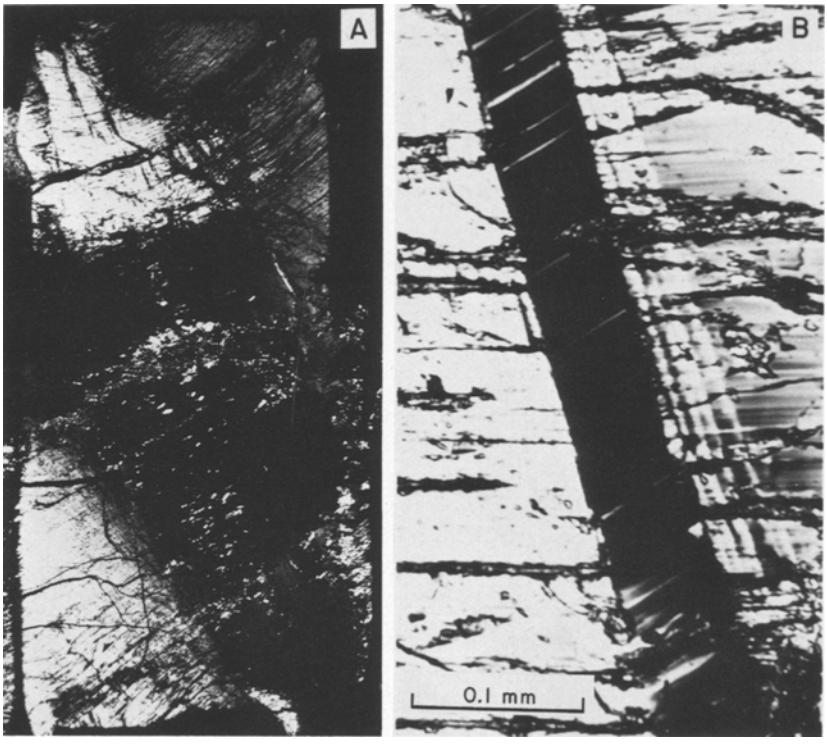

Fig. 9. (A) Reversion of CE to OE by annealing at 1100°C, 16.5 kb and approximately zero differential stress for 80 min. Reverted (center) and original (top) OE are both near extinction; unreverted CE (light) remains at the cooler ends. Note small kinks in CE at upper left which we believe formed by extension of the specimen during reversion. Before annealing this core (6 mm diameter) shortened 20 percent at 10^{-4} sec^{-1}, 800°C and 16.5 kb. (B) Close-up of one of the kinks in the upper left of (A) containing reverted OE (at extinction). Both (A) and (B) are (010) sections under crossed nicols with *c*-axis parallel to prominent lineations (NE-SW to E-W)

temperatures, pressures, and compositions (approximately $En_{86}Fs_{14}$) it is probable that only the stability field of OE was entered, *i.e.*, that the stability fields of protoenstatite and high-clinoenstatite were avoided (Boyd *et al.*, 1964; Smyth, 1974 and personal communication). Complete reversion of CE to OE occurred during annealing for a few hours in those portions of the specimens where temperatures were 950°C or more, and the OE so produced also has a^*-, *b*-, and *c*-axes parallel to those of the remaining CE, as does the OE near the end pieces which was never transformed (Fig. 9A). Reversion in these experiments was much quicker than the reversion at 1 atm pressure described above. We believe this difference is due to the catalyzing effect of water released by the dehydration of the talc confining medium during annealing, maybe by increasing the mobility of the transformation partials by the same mechanism that causes water-weakening in silicates (Griggs, 1967; Blacic, 1972).

As in the experiments at 1 atm, the reversion of CE to OE in these experiments was noticeably time dependent at all temperatures for which it was observed. At 1200°C it takes place very quickly, but not instantaneously. Figure 1 (right) shows that reversion is only partially complete after annealing at 1200°C for about 30 seconds.

In these experiments the specimens obviously did not recover their original shape as a result of transformation back to OE [Fig. 1 (right) and 9A]. This is not just because the specimens also deformed by slip; there was very little recovery of the transformation strain during reversion from CE to OE. The only exceptions to this were small kinks near the cold ends of the specimen in which the sense of rotation indicated extension parallel to the axis of former compression (Fig. 9B). The irreversibility of the transformation strain manifested in most of the specimen probably does not mean that a different transformation mechanism was operative. Rather, we think that the reversion of CE to OE was accomplished by exactly the reverse of the mechanism which accomplishes the transformation of OE to CE, but that stresses arising from the constraints caused by the strength of the con-confining medium and the rigid end pieces caused compensatory slip in the OE and CE which just nullified the transformation strain of reversion.

Transmission Electron Microscopy. Examination of foils of reverted enstatite by TEM supports the hypothesis of compensatory slip during reversion. Fig. 10 shows in (010) orientation three stages in the reversion of CE to OE. The first (Fig. 10A) is from the specimen annealed at 1200°C for 30 seconds [see the thin sections in Fig. 1 (right)], and is from a region which is apparently transitional between the two phases. The bright field micrograph is exceedingly complex and the diffraction pattern is streaked, distorted, and not recognizable as either OE, CE, or a simple combination of the two. The second (Fig. 10B) is from the same specimen in what appeared under the light microscope to be entirely reverted OE. The electron diffraction pattern suggests that both OE and CE are present, and the micrograph shows that there are many dislocations as well. The third (Fig. 10C) is from a different specimen that was annealed for 80 minutes at 1100°C (see Fig. 9A for thin section), and reversion is essentially complete. The diffraction pattern is that of OE and is only very slightly streaked; the micrograph shows OE with relict stacking faults and numerous unit dislocations.

Contrast studies of foils of reverted OE in the off-(100) orientation (Fig. 11) reveal that most of these unit dislocations belong again to the slip system (100) [001] (Table 1), just as they did for CE. There is, however, a significant difference; the dislocations in the reverted OE are dominantly screw while those in the deformed CE are of mixed character. We conclude that these features indicate slip did occur during the process of reversion, and that the predominance of dislocations on the system (100) [001] supports the contention that the transformation shear associated with reversion is essentially cancelled by slip.

Further Discussion

Thermodynamics

If we knew the effect that shear stress has on the temperature of equilibrium between OE and CE, then the natural occurrences of CE in OE might be used to

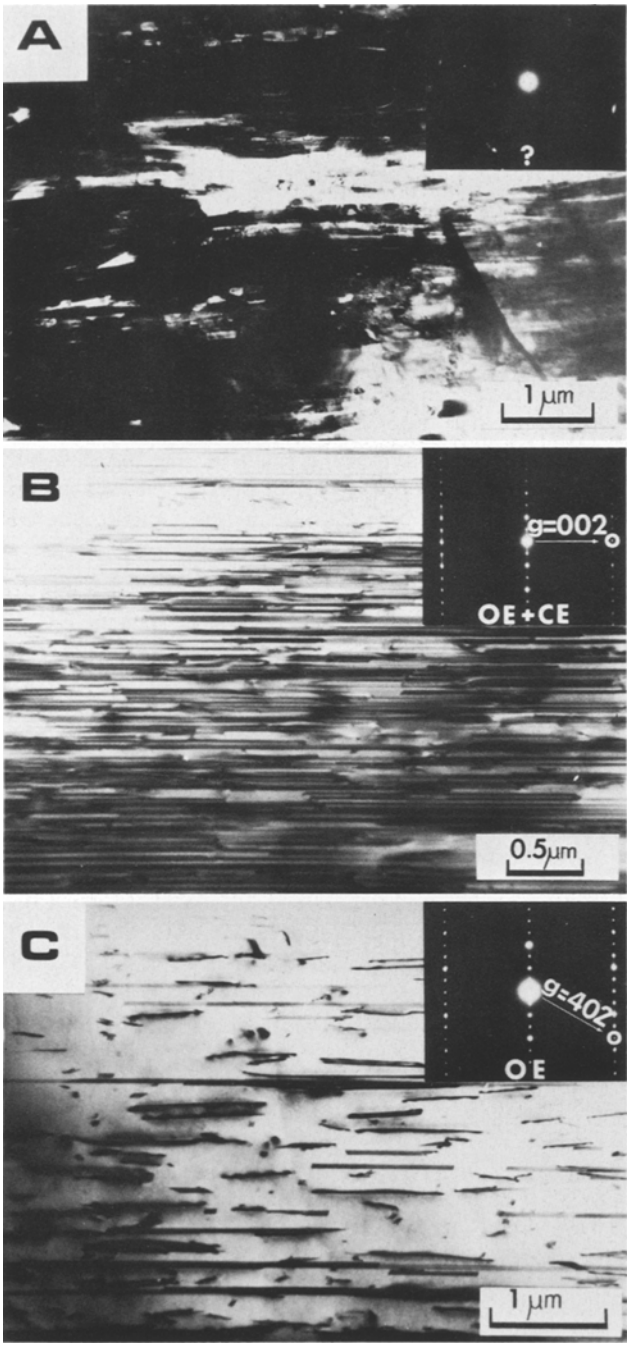

Fig. 10A—C. BF electron micrographs of (010) foils of deformed specimens which show different degrees of reversion by annealing ([001] E-W). (A) Unrecognizable transitional phase that was between clearly reverted OE and unreverted CE in specimen annealed about 30 sec at 1200° C. (B) Partial reversion to OE in different portion of same specimen as (A). (C) Complete reversion to OE in foil from same specimen as Fig. 9 annealed for 80 min at 1100° C. Note the abundance of unit dislocations

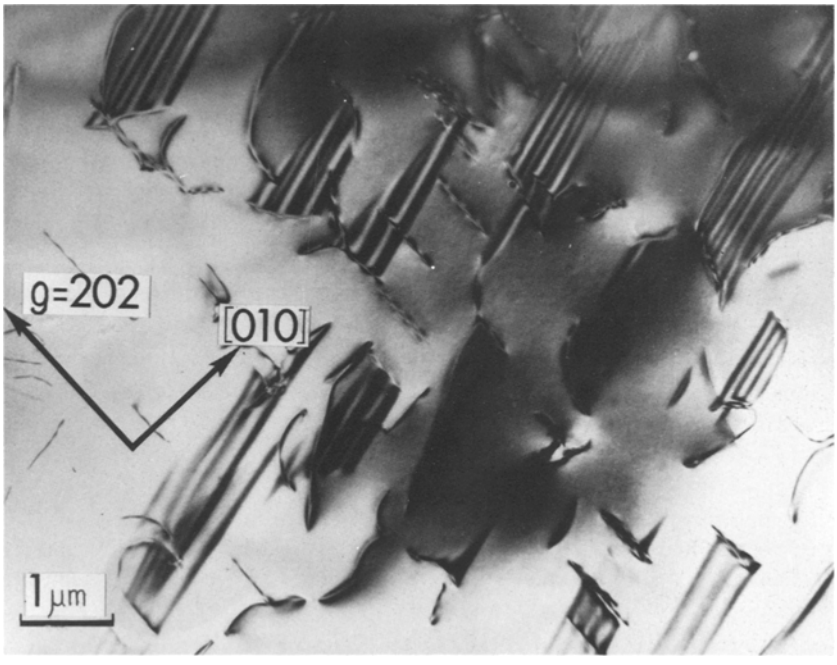

Fig. 11. BF electron micrograph of reverted OE in foil of off-(100) orientation from same specimen as Fig. 9 and 10C. Both unit and partial dislocations belong to the slip system (100) [001] (see Table 1) and show some preference in alignment parallel to [001]

say something about the magnitude of shear stress in the earth's crust. At the moment we can make only semi-quantitative estimates, but it is encouraging that a number of different approaches lead to roughly similar results. All the estimates depend in part on Grover's (1972a and b and personal communication) hydrostatic phase boundary: $T = 566°\text{C} + (4.5°\text{C/kb})\,P$.

Our deformation experiments at 5 kb confining pressure show that about 1 kb shear stress on (100) parallel to [001] is more than sufficient to cause OE to invert to CE at temperatures up to at least 850°C. By Grover's data the equilibrium temperature at 5 kb confining pressure and zero shear stress should be about 590°C, assuming that to a first approximation the effect on equilibrium of the 14 mol percent ferrosilite in solid solution in our specimens can be neglected. Therefore, an approximate lower bound for the slope of the phase boundary between $\tau_r = 0$ and $\tau_r = 1$ kb shear stress resolved on (100) planes in the direction of [001] is $\mathrm{d}T/\mathrm{d}\tau_r > 260°\text{C/kb}$. Besides the unknown amount of overstepping of the transition boundary due to the kinetics of the OE to CE transformation, $\mathrm{d}T/\mathrm{d}\tau_r$ is only approximate because of undertainty of the state of stress due to friction, the strength of the solid medium, and inhomogeneities as well as uncertainty in the temperature at points away from the thermocouple junction.

A different calculation involves Grover's equilibrium temperature $T_0 = 566°\text{C}$ and an estimate of the enthalpy difference $\Delta h \cong 600$ cal/mole between OE and CE (I. S. E. Carmichael, personal communication) that is based on the dis-

crepancies caused by using thermodynamic data derived from CE in thermodynamic calculations for mineralogical reactions that actually involve OE. This corresponds to an entropy difference of about $\Delta s \cong 0.7$ cal/mole-°K. Using this value and $\psi = 13.3°$ for the angle of transformation shear in the theoretical expression derived by Coe (1970)

$$dT/d\tau_r = v \tan\psi / \Delta s \quad (1)$$

yields an estimate of 250°C/kb for the slope of the phase boundary.

Yet another method is to use estimates of the molar volume difference Δv and Grover's dT/dP to solve for Δs in the Clapeyron equation, which is then substituted into (1), just as in the previous method. Stephenson *et al.* (1966) found a very small value of 0.015 cm³/mole from OE and CE that was synthesized at high pressure in a solid medium apparatus. Burnham (1965) found $\Delta v = 0.056$ cm³/mole for synthetic orthoferrosilite and clinoferrosilite. Turnock *et al.* (1973) obtained $\Delta v = 0.07$ cm³/mole for synthetic OE and CE, and, most recently, Grover (personal communication) finds $\Delta v = 0.1$ cm³/mole for OE and CE coexisting in metamorphic rocks in she Swiss Alps (Grover, 1972a, b). Using Grover's value for the natural OE and CE, we calculate a value of $dT/d\tau_r = 330°C$/kb, whereas the much smaller value of Δv of Stephenson *et al.* would yield a figure almost 7 times as great.

In summary, there is a comforting, though perhaps fortuitous, clustering of estimates of $dT/d\tau_r$ around 300°C per kilobar of shear stress on (100) planes in the [001] direction. Grover's values for T_0, dT/dP, and Δv, Carmichael's estimate of Δh, and our lower bound for $dT/d\tau_r$ are thermodynamically consistent within about ± 25 percent. Better direct determinations of $dT/d\tau_r$ are needed, including reversals of the phase boundary while the specimen is under stress, in order to be sure whether this agreement is meaningful. It will also be necessary to assess the effects of compositional variations on the phase boundary.

OE-CE Geopiezometer?

Raleigh *et al.* (1971) showed by deforming natural polycrystalline specimens of OE that at a given temperature there is a narrow range of strain rates above which the dominant mode of deformation occurs by transformation and below which it occurs by slip. They determined the boundary between the two deformation mechanisms in terms of tempertaure and strain rate between 900 and 1400°C and 10^{-7} and 10^{-2} sec^{-1}. These experiments established the potential for using the occurrence of CE in rocks to set a lower bound on the strain rate at the time of formation of the CE if the temperature could be independently estimated. By extrapolating their results they concluded that usual geologic strain rates of 10^{-13} to 10^{-15} sec^{-1} were insufficient to allow transformation at temperatures greater than about 600°C, and they suggested that this might explain the rarity of CE in naturally deformed rocks.

Similarly, the OE-CE transition could potentially enable estimation of the stresses operating in nature. If the transition is to be useful as a geopiezometer, however, CE must be produced by shear in a variety of rocks and persist throughout the subsequent history of the rocks. As mentioned in the introduction, such CE

has been found in terrestrial rocks with somewhat greater frequency during the last few years. It may well have been mistaken for exsolution in the past before high-resolution electron probes and microscopes were available. If so, we should expect new discoveries of CE produced by shear in nature to continue.

Whether CE persists in a rock after it is formed depends on the stress and cooling history of the rock and the kinetics of the reverse transition from CE to OE. The kinetics probably depend not only on temperature, but also on the presence of water, the constraints at grain boundaries, and the state of internal strain and stress. In our experiments in which we heated dry single crystals containing CE lamellae in OE we detected optically very slight but definite reversion within a few hours around 1000°C. With single-crystal X-ray techniques Smyth (1974) found significant reversion within a few hours at temperatures as low as 800°C. His CE was produced by quenching enstatite rather than by deformation, and this may well make a difference. Our deformation experiments suggest negligible reversion in single crystals within a few hours at 800°C dry, and significant reversion at 850 to 900°C in the presence of small amounts of water supplied by the dehydration of the talc confining medium. In dry *polycrystalline* enstatite-bearing rocks the rates of reversion of shear-induced CE appear to be slower than in single crystals. Raleigh (1967) reported no signs of reversion after heating for 170 hours at 850°C and atmospheric pressure, and Raleigh *et al.* (1971) had no difficulty preserving CE produced in deformation experiments at temperatures to 1200°C, even though the high temperatures were maintained during the few minutes that it took to decrease the differential stress to zero at the end of the runs. Thus, it seems possible that CE may persist in nature for long times under dry conditions even at temperatures well above 800°C.

Under favorable conditions, the orientations of OE grains which have CE lamellae in them should enable one to estimate the orientation of the principal axes of the stress field which caused the CE to form in the rock. One would employ exactly the same principles that are used in the dynamic analysis of twinning (Turner, 1953; Raleigh and Talbot, 1967; Carter and Raleigh, 1969). The main difference is that shear on (100) [001] of OE promotes the formation of a different polymorph (CE) rather than a twin. This difference provides the conceptual basis for estimating the *magnitude* of the principal stresses as well, to which we now turn.

First we consider the simple case of biaxial compression with principal stresses $\sigma_1 > \sigma_2 = \sigma_3$ and compressive stresses defined positive. The magnitude of the shear stress on any plane whose normal is inclined at an angle θ to x_1 (the direction of σ_1) is

$$\tau = \tfrac{1}{2}(\sigma_1 - \sigma_3)\sin 2\theta. \tag{2}$$

It is maximum when $\theta = 45°$ and falls off symmetrically for larger or smaller values of θ. Thus if all possible orientations of OE grains were represented in the rock and if the maximum value of the shear stress exceeded the shear stress on (100) resolved parallel to [001] that is required for OE-CE equilibrium ,τ_r', then the a^*-axes of OE grains in which CE lamellae formed should lie in a girdle about x_1 centered on the small circle with $\theta = 45°$. Note that not all OE grains with a^*-axes within the girdle will transform, however, because τ_r, the shear stress on

(100) resolved parallel to [001], will vary from zero to τ depending on the orientation of the grain. The angular width of the girdle, $\Delta\theta$, will be limited by the condition that no CE can form if $\tau < \tau_r'$. Assuming that equilibrium is attained at the edge of the girdle ($\tau = \tau_r'$), we have from (2)

$$\tau = \tfrac{1}{2}(\sigma_1 - \sigma_3)\sin 2(45° \pm \Delta\theta/2) = \tau_r'$$

so that

$$\sigma_1 - \sigma_3 = \frac{2\tau_r'}{\cos\Delta\theta} \tag{3}$$

If the temperature and mean pressure during formation of CE can be estimated independently from, say, other geochemical or petrographic data, then knowledge of the $T - \tau_r$ phase boundary would enable one to estimate the equilibrium resolved shear stress τ_r'. This and the measured width of the girdle, $\Delta\theta$, would in turn allow one to estimate the principal stress difference $(\sigma_1 - \sigma_3)$ from Eq. 3.

More general, triaxial stress distributions do not greatly complicate the conceptual method. First determine the orientation of the principal axes by, for instance, the method of Raleigh and Talbot (1967). Then estimate the principal stress differences by

$$\sigma_1 - \sigma_3 = \frac{2\tau_r'}{\cos\Delta\theta_{13}} \tag{4a}$$

$$\sigma_1 - \sigma_2 = \frac{2\tau_r'}{\cos\Delta\theta_{12}} \tag{4b}$$

$$\sigma_2 - \sigma_3 = \frac{2\tau_r'}{\cos\Delta\theta_{23}} \tag{4c}$$

where $\Delta\theta_{13}$, $\Delta\theta_{12}$, and $\Delta\theta_{23}$ are the angular ranges measured in the three principal planes of a^*-axes of OE grains which contain CE lamellae. Only two of Eqs. 4a, 4b, and 4c are independent; equating the sum of (4b) and 4c) to (4a) yields an equation which can serve as a measure of the consistency of the analysis:

$$\frac{1}{\cos\Delta\theta_{13}} = \frac{1}{\cos\Delta\theta_{12}} + \frac{1}{\cos\Delta\theta_{23}} \tag{5}$$

The mean pressure is by definition

$$\bar{P} = \tfrac{1}{3}(\sigma_1 + \sigma_2 + \sigma_3) \tag{6}$$

which, when combined with Eqs. (4a), (4b), and (4c), yields the estimates of the magnitudes of the principal stresses themselves:

$$\sigma_1 = \bar{P} + \frac{2\tau_r'}{3}\left(\frac{1}{\cos\Delta\theta_{12}} + \frac{1}{\cos\Delta\theta_{13}}\right) \tag{7a}$$

$$\sigma_2 = \bar{P} + \frac{2\tau_r'}{3}\left(\frac{-1}{\cos\Delta\theta_{23}} + \frac{1}{\cos\Delta\theta_{12}}\right) \tag{7b}$$

$$\sigma_3 = \bar{P} - \frac{2\tau_r'}{3}\left(\frac{1}{\cos\Delta\theta_{13}} + \frac{1}{\cos\Delta\theta_{23}}\right) \tag{7c}$$

Raleigh and Talbot (1967) have demonstrated that the orientation of the principal stresses can be deduced rather well by fabric analyses of rocks containing

mechanically twinned diopside. Assuming that this could be done for rocks containing mechanically transformed OE as well, there are still additional uncertainties associated with the determination of the magnitudes of the principal stresses. There is the question of kinetics with regard to the assumption of equilibrium between OE and CE; if equilibrium were not attained, the estimated stress differences would be too low. This may not be too serious a problem, though, because shear stress increases the reaction rates so drastically that very little overstepping of the phase boundary may be necessary in order to form CE within geologically relevant times. Another problem involves the independent estimates of temperature and pressure. If the true value of $dT/d\tau_r$ is in fact about what we estimate (approximately 300°C/kb), then an error of 75°C in the temperature estimate would cause an error of at least 0.5 kb in the principal stress differences. The pressure estimate is not nearly so critical, an error of 1 kb leading to an error in the stress differences of the order of 0.05 kb. In addition, the effects of compositional variations on the slope and intercept of the phase boundary remain to be determined and, in some cases, might be substantial. The most serious problem, however, may well be the non-uniformity of stress from grain to grain that arises from the elastic inhomogeneity and grain-boundary constraints in polycrystalline solids. One should probably omit from the fabric analysis grains in which CE formed in kinks and use only the OE grains which contain lamellae. Nonetheless, stress variations will still be a factor in these remaining grains, increasing the angular ranges of orientations of grains in which transformation occurred and thus causing an overestimation of the average principal stress differences which operated on the rock as a whole.

Clearly, the effects of these and other sources of errors must be assessed by additional experiments and observations of natural occurrences of clinoenstatite-bearing rocks before the usefulness of the method can be known.

Acknowledgements. We acknowledge J. M. Christie and the late D.T. Griggs for their helpful discussions. R. S. C. received financial support from NSF Grant GA-25165, an Alfred P. Sloan Foundation Research Fellowship, and a UCSC Faculty Research Grant. S. H. K. acknowledges support from NSF Grants GA-26027 and GA-36077.

References

Amelinckx, S.: The study of planar interfaces by means of electron microscopy. In: Modern diffraction and imaging techniques in material science, S. Amelinckx, R. Gevers, G. Remaut, J. Van Landuyt, eds., p. 257–294. Amsterdam-London-New York: North Holland/American Elsevier 1970

Blacic, J.D.: Effect of water on the experimental deformation of olivine. In: Flow and fracture in rocks, H. C. Heard, I. Y. Borg, N. L. Carter, C. B. Raleight, eds., Am. Geophys. Union Geophysical Monograph 16, p. 109–115. Richmond: William Byrd Press 1972

Boland, J.N.: Electron petrography of exsolution in an enstatite-rich orthopyroxene. Contrib. Mineral. Petrol. **37**, 229–234 (1972)

Boland, J.N.: Lamellar structures in low-calcium orthopyroxenes. Contrib. Mineral. Petrol., **47**, 215–222 (1974)

Borg, I., Handin, J.: Experimental deformation of crystalline rocks. Tectonophysics **3**, 249 (1966)

Boyd, F.R., England, J.L.: The rhombic enstatite-clinoenstatite inversion. Carnegie Inst. Wash. Yrbk. **64**, 117–120 (1965)

Brown, W.L., Morimoto, N., Smith, J.V.: A structural explanation of the polymorphism and transitions of $MgSiO_3$. J. Geol. **69**, 609–616 (1961)

Burnham, C.W.: Ferrosilite. Carnegie Inst. Wash. Yrbk. **64**, 202–204 (1965)

Burnham, C.W.: Ferrosilite. Carnegie Inst. Wash. Yrbk. **65**, 285–290 (1967)

Buseck, P.R., Iijima, S.: High resolution electron microscopy of silicates. Am. Mineralogist **59**, 1–21 (1974)

Carter, N.L., Raleigh, C.B.: Principal stress directions from plastic flow in crystals. Geol. Soc. Am. Bull. **80**, 1231–1264 (1969)

Champness, P.E., Lorimer, G.W.: Precipitation (exsolution) in an orthopyroxene. J. Materials Sci. 8, 467–474 (1973)

Champness, P.E., Lorimer, G.W.: A direct lattice-resolution study of precipitation (exsolution) in orthopyroxene. Phil. Mag. **30**, 357–365 (1974)

Coe, R.S.: The thermodynamic effect of shear stress on the ortho-clino inversion in enstatite and other phase transitions characterized by a finite simple shear. Contrib. Mineral. Petrol. **26**, 247–264 (1970)

Coe, R.S., Müller, W.F.: Crystallographic orientation of clinoenstatite produced by deformation of orthoenstatite. Science **180**, 64–66 (1973)

Deer, W.A., Howie, R.A., Zussman, J.: Rock forming minerals, vol. 2, Chain silicates. London: Longmans 1963

Frost, B.R.: Contact metamorphism of the Ingalls Complex at Paddy-Go-Easy-Pass, Central Cascades, Washington. Ph.D. Thesis, University of Washington, Seattle, Washington (1973)

Green, H.W., Griggs, D.T., Christie, J.M.: Syntectonic recrystallization and annealing of quartz aggregates. In: Experimental and natural rock deformation, p. 272–335. Berlin-Heidelberg-New York: Springer 1970

Green, H.W., Radcliffe, S.V.: Deformation processes in the upper mantle. In: Flow and fracture of rocks, H. C. Heard, I. Y. Borg, N. L. Carter, C. B. Raleigh, eds., Am. Geophys. Union Geophysical Monograph 16, p. 139–156. Richmond: William Byrd Press 1972

Griggs, D.T.: Hydrolytic weakening of quartz and other silicates. Geophys. J. Roy. Astron. Soc. **14**, 19–31 (1967)

Grover, J.E.: Two problems in pyroxene mineralogy: A theory of partioning of cations between coexisting single and multi-site phases; and a determination of the stability of low-clinoenstatite under hydrostatic pressure. Ph.D. thesis, 327 p.: Yale University 1972a

Grover, J.E.: The stability of low-clinoenstatite in the system $Mg_2SiO_2O_6$—$CaMgSi_2O_6$. EOS, Trans. Am. Geophys. Union **53**, 539 (1972b)

Kirby, S.H.: The role of crystal defects in the shear-induced transformation of orthoenstatite to clinoenstatite. In: Applications of electron microscopy in mineralogy, J. M. Christie, J. Cowley, A. Heuer, G. Thomas, N. Tighe, H.-R. Wenk, eds. Berlin-Heidelberg-New York: Springer 1975 (in press)

Kohlstedt, D.L., Vander Sande, J.B.: Transmission electron microscopy investigation of the defect microstructure of four natural orthopyroxenes. Contrib. Mineral. Petrol. **42**, 169–180 (1973)

Lally, J.S., Fisher, R.M., Christie, J.M., Griggs, D.T., Heuer, A.H., Nord, G.L., Radcliffe, S.V.: Electron petrography of Apollo 14 and 15 rocks. In: Proc. 3rd Lunar Sci. Conf., Geochimica Cosmochimica Acta, Suppl. 3, vol. 1, p. 401–422. M.I.T. Press 1972

Lindsley, D.H., Munoz, J.L.: Ortho-clino inversion in ferrosilite. Carnegie Inst. Yrbk. **67**, 86–88 (1969)

Lorimer, G.W., Champness, P.E.: Combined electron microscopy and analysis of an orthopyroxene. Am. Mineralogist **58**, 243–248 (1973)

Morimoto, N., Koto, K.: The crystal structure of orthoenstatite. Kristallogr. **129**, 66–83 (1969)

Müller, W.F.: One-dimensional lattice imaging of a deformation-induced lamellar intergrowth of orthoenstatite and clinoenstatite [(Mg, Fe)SiO_3]. Neues Jahrb. Mineral. Mg. **2**, 83–88 (1974)

Raleigh, C.B.: Plastic deformation of upper mantle silicates. Geophys. J. **14**, 45–49 (1967)

Raleigh, C.B., Talbot, J.L.: Mechanical twinning in naturally and experimentally deformed diopside. Am. J. Sci. **265**, 151–165 (1967)

Raleigh, C.B., Kirby, S., Carter, N.L., Avé Lallemant, H.G.: Slip and the clinoenstatite transformation as competing rate processes in enstatite. J. Geophys. Res. **76**, 4011–4022 (1971)

Riecker, R.E., Rooney, T.P.: Deformation and polymorphism of enstatite under shear stress. Geol. Soc. Am. Bull. **78**, 1054–1054 (1967)

Sadanaga, R., Okamura, F.P., Takeda, H.: X-ray study of the phase transformations of enstatite. Mineral. J. **6**, 110–130 (1969)

Sclar, C.B., Carrison, L.C., Schwartz, C.M.: High-pressure stability field of clinoenstatite and the orthoenstatite-clinoenstatite transition. Trans. Amer. Geophys. Union **45**, 121 (1964)

Smith, J.V.: Crystal structure and stability of the $MgSiO_3$ polymorphs: physical properties and phase relations of Mg—Fe pyroxenes. In: Pyroxenes and amphiboles, crystal chemistry and phase petrology, J. J. Papike, ed., Mineral. Soc. Am. Spec. Papers **2**, 3–30 (1969)

Smyth, J.R.: Experimental study on the polymorphism of enstatite. Am. Mineralogist **59**, 345–352 (1974)

Starkey, J.: The geometry of kink bands in crystals—a simple model. Contrib. Mineral. Petrol. **19**, 133–141 (1968)

Stephenson, D.A., Sclar, C.B., Smith, J.V.: Unit cell volumes of synthetic orthoenstatite and low clinoenstatite. Mineral. Mag. **35**, 838–846 (1966)

Trommsdorff, V., Wenk, H.R.: Terrestrial metamorphic clinoenstatite in kinks of bronzite crystals. Contrib. Mineral. Petrol. **19**, 158–168 (1968)

Turner, F.J.: Nature and dynamic interpretation of deformation lamellae in calcite of three marbles. Am. J. Sci. **251**, 276–298 (1953)

Turner, F.J., Heard, H., Griggs, D.T.: Experimental deformation of enstatite and accompanying transformation to clinoenstatite. Int. Geol. Congr., 21st, Copenhagen, Part 18, 399–408 (1960)

Turnock, A.C., Lindsley, D.H., Grover, J.E.: Synthesis and unit cell parameters of Ca—Mg—Fe pyroxenes. Am. Mineralogist **58**, 50–59 (1973)

Vander Sande, J.M., Kohlstedt, D.L.: A high-resolution electron microscopy study of exsolution lamellae in enstatite. Phil. Mag. **29**, 1041–1049 (1974)

Weiss, L.E., Turner, F.J.: Some observations on translation gliding and kinking in experimentally deformed calcite and dolomite. In: Flow and fracture in rocks, H. C. Heard, I. Y. Borg, N. L. Carter, C. B. Raleigh, eds., Am. Geophys. Union Geophysical Monograph 16, p. 95–107. Richmond: William Byrd Press 1972

Dr. R. S. Coe
Earth Sciences Board
University of California
Santa Cruz, California 95604, U.S.A.